Novel ^{18}F labeling strategy for polyester-based NPs for *in vivo* PET-CT imaging

Primiano Pio Di Mauro [1,2], Vanessa Gómez-Vallejo [4], Zuriñe Baz Maldonado [3], Jordi Llop Roig [3,*], Salvador Borrós [1,2,]**

1 Sagetis-Biotech;, Barcelona

2 Grup d'Enginyeria de Materials (GEMAT), Institut Quimic de Sarria, Universidad Ramon Llull,

3 Radiochemistry and Nuclear imaging, CIC biomaGUNE, San Sebastian, Spain.

4 Radiochemistry Department, CIC biomaGUNE, San Sebastian, Spain

*Co-corresponding author jllop@cicbiomagune.es
** Co-corresponding author salvador.borros@iqs.url.edu

ABSTRACT

Drug-loaded nanocarriers and nanoparticulate systems used for drug release require a careful *in vivo* evaluation in terms of physicochemical and pharmacokinetic properties. Nuclear imaging techniques such as Positron Emission Tomography (PET) are ideal and non-invasive tools to investigate the biodistribution and biological fate of the nanostructures, but the incorporation of a positron emitter is required. Here we describe a novel approach for the ^{18}F-radiolabeling of polyester-based nanoparticles. Our approach relies in the preparation of the radiolabeled active agent 4-[^{18}F]fluorobenzyl-2-bromoacetamide ([^{18}F]FBBA), which is subsequently coupled to block co-polymers under mild conditions. The labeled block co-polymers are ultimately incorporated as constituent elements of the NPs by using a modified nano co-precipitation method. This strategy has been applied in the current work to the preparation of peptide-functionalized NPs with potential applications in drug delivery. According to the measurements of particle size and zeta potential, the radiolabeling process did not result in a statistically significant alteration of the physic-chemical properties of the NPs. Moreover, radiochemical stability studies showed no detachment of the radioactivity from NPs even at 12 hours after preparation. The radiolabeled NPs enabled the *in vivo* quantification of the biodistribution data in rats using a combination of imaging techniques, namely PET and Computerized Tomography (CT). Low accumulation of the nanoparticles in the liver and their elimination mainly via urine was found. The different biodistribution pattern obtained for the "free" radiolabelled polymer suggests chemical and radiochemical integrity of the NPs under investigation. The strategy here reported may be applied to any polymeric NPs containing polymers bearing a nucleophile, and hence our novel strategy may find application for the *in vivo* and non invasive investigation of a wide range of NPs.

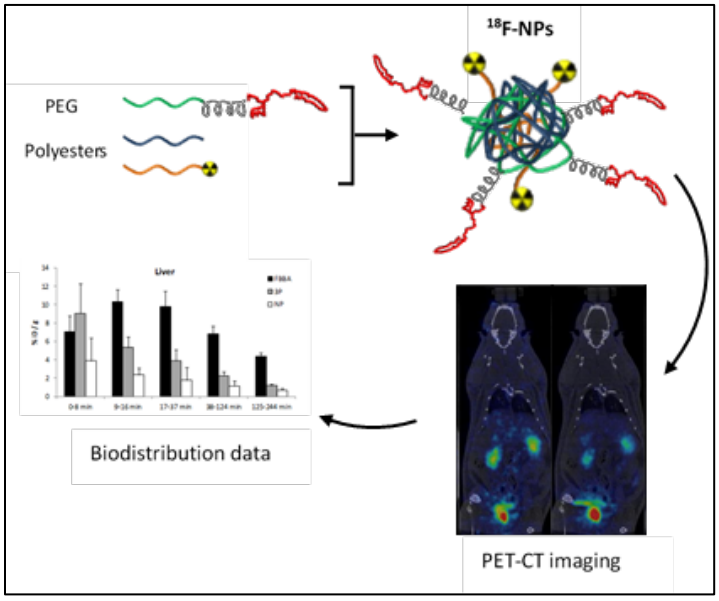

INTRODUCTION

Nanomaterials (NMs) can be broadly classified as organic/polymeric, carbon based, inorganic and hybrid. Inorganic NMs can have very different surface-to-volume ratios and shapes[1,2] and are ubiquitously utilized as food or paint additives,[3,4] in the construction and semi-conductor industries,[5,6] in cosmetic applications[7] and in many other industrial and societal sectors. Carbon based NMs formed by carbon in sp2 conformation have recently gained significant attention for their potential applications in a varied range of industries such as spintronics,[8,9] and sensor development.[10,11] Organic/polymeric NMs are frequently applied in nanomedicine.[12] Finally, hybrid NMs combine materials of different nature, e.g. as core/shell NMs or hierarchical structures, leading thus to a limitless number of scenarios in terms of chemical composition, potential complexity of the NMs and their applications.

Among NMs, polymer based nanoparticles (PNPs) have been proposed as suitable drug delivery vehicles. Since many drugs and therapeutic agents have poor pharmacokinetic properties, their entrapment into PNPs can be anticipated as a valuable alternative to enhance their therapeutic worth by improving their bioavailability, solubility in physiological environment or circulation time.[13,14] Additionally, carrier NPs can enable delayed drug release and improve selective accumulation in specific tissues, by attachment of specific targeting moieties on the NPs surface.

Nanocarriers designed for the selective delivery of drugs to specific tissues or organs after systemic administration require long circulation times in the bloodstream, in order to reach the targeted organ or tissue before clearance or degradation occurs.[15–18] This is not likely to happen if the carrier is taken up by the mononuclear phagocyte system (MPS, also called reticuloendothelial system or RES) immediately after intravenous administration, or if rapid renal excretion occurs. Similar considerations are needed for nanosystems meant to be a circulating reservoir for sustained release of therapeutic cargoes. Hence, investigation of the pharmacokinetic properties of PNPs with biomedical applications is of paramount importance.

Different approaches can be used to investigate the pharmacokinetic properties of PNPs. Invasive visualization methods such as optical or electron microscopies are often employed. Alternatively, *in vivo* imaging techniques such as Positron Emission Tomography (PET), Single Photon Emission Computerized Tomography (SPECT), Magnetic Resonance Imaging (MRI) or Fluorescence Tomography can also be applied. Among them, PET offers unparalleled *in vivo* sensitivity; in addition, due to the high penetration capacity of the high-energy (511 keV) gamma rays resulting from positron annihilation, it can be applied both to small and large animal species as well as humans. Hence, PET represents an ideal tool to investigate, *in vivo* and non-invasively, the biological fate of NPs, including stability in biological environments (stealthiness), pharmacokinetics, and specific organ uptake.[19]

The investigation of the pharmacokinetic properties of NPs using PET requires the incorporation of a positron emitter in the NP (radiolabeling). To date, different PNP-radiolabeling strategies have been developed, being attachment of a radiometal (e.g., ^{68}Ga or ^{64}Cu)[20,21] by means of a bifunctional chelator (BFC) the most commonly used. Despite very useful in a wide variety of scenarios, attachment of a radionuclide using BFCs has several drawbacks. First, the formation of the chelator-radiometal complex may be hampered if the chelators (which are usually attached to the NPs during preparation) are sterically hindered or not accessible. Second, the presence of non radioactivce metals with the capacity to form complexes with the chelator all along the production process may compromise the radiochemical yields and the specific radioactivity of the resulting radiolabeled PNPs. Finally, release of the radiometal or transchelation due to the presence

of certain proteins during *in vivo* investigations may lead to completely wrong conclusions, as the presence of the free radionuclide might be mistakenly interpreted as a signature of the PNPs presence.

One alternative to the use of radiometals consists of radiolabeling the NPs with ^{18}F, a relatively long half-lived positron emitter ($T_{1/2}$ = 109.7 min), which can be produced as $[^{18}F]F^-$ in the GBq scale in all biomedical cyclotrons. Unfortunately, direct labeling with $[^{18}F]F^-$ requires harsh conditions (for example, high temperature and water-free organic solvent), and long reaction times;[22] alternatively, indirect labeling methods can be used. In these, a radiolabeled prosthetic group is prepared in a first step and subsequently coupled to the molecule of interest, usually under mild conditions. This strategy has been applied to the preparation of radiolabelled NPs;[23,24] of note, the presence of a reactive group on the surface of the NPs able to react with the labeled prosthetic group is required, and hence this strategy cannot be directly translated to certain types of polymeric NPs. The development of alternative synthetic routes is thus particularly convenient.

Very recently, we have reported the preparation of Paclitaxel-loaded PNPs using a modified nanoprecipitation method.[25] In this work, and following a similar synthetic strategy, we present an unprecedented strategy for the preparation of analogous radiolabeled PNPs. Our method relies on radiolabeling block co-polymers using the labeling agent 4-[^{18}F]fluorobenzyl-2-bromoacetamide ([^{18}F]FBBA). These block co-polymers are ultimately incorporated in the PNPs as constituent elements. The strategy has been applied to the preparation of radiolabeled, peptide-functionalized PNPs with potential applications in drug delivery. Finally, quantitative biodistribution data was obtained *in vivo* after intravenous administration in rodents using a combination of imaging techniques. The strategy reported here relies in the condensation of the labeling agent [^{18}F]FBBA with a polymer containing a nucleophile, and subsequent utilization of the labeled polymer for the preparation of radiolabeled NPs. Hence, our approach may find application in the preparation of a wide range of radiolabelled polymeric NPs, and become thus an interesting tool for the evaluation of the pharmacokinetic properties of newly developed PNPs.

RESULTS AND DISCUSSION

Synthesis and characterization of [^{18}F]FBBA and ^{18}F-labeled polymers

The labeled active agent [^{18}F]FBBA was synthesized following a well established 3-step procedure (Figure 1).[26] First, 4-[^{18}F]fluorobenzonitrile ([^{18}F]**2**) was prepared by reaction of 4-Cyano-*N*,*N*,*N*-trimethylanilinium trifluoromethanesulfonate (**1**) with [^{18}F]F^-. After purification using solid phase extraction and water removal using Na_2SO_4 and molecular sieve, the cyano group in [^{18}F]**2** was efficiently reduced with $LiAlH_4$ to yield [^{18}F]**3**, which was further reacted with bromoacetyl bromide to yield [^{18}F]**4.** After purification using HPLC, the presence of the desired labeled species was confirmed by HPLC and co-elution with reference standard (Figure 2). Radiochemical yields similar to those previously reported in the literature (12%, decay corrected; total synthesis time approximately 90 min including purification) were achieved.

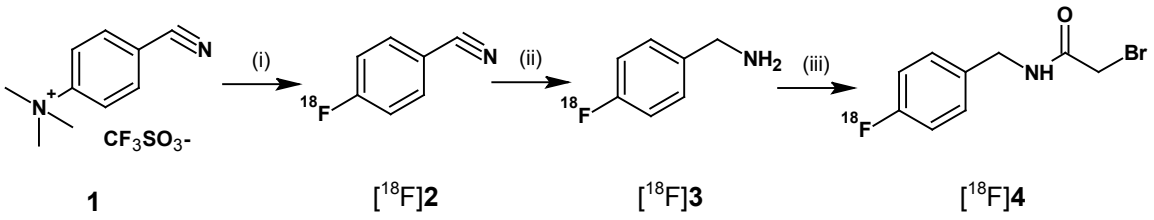

Figure 1 Scheme of the reaction for the preparation of [^{18}F]FBBA ([^{18}F]**4**); (i) azeotropically dried [^{18}F]F^-, K_2CO_3, $K_{2.2.2.}$, MeCN, 130°C, 10 min; (ii) 0.1M $LiAlH_4$, 2 min, 120 °C; (iii) bromoacetyl bromide in CH_2Cl_2, 2 min, RT.

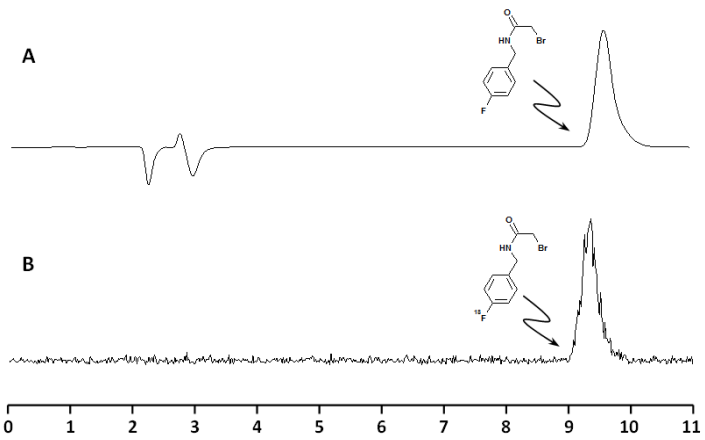

Figure 2 HPLC chromatograms corresponding to: A) FBBA (reference standard solution, UV detector) and B) [^{18}F]FBBA (purified fraction, radiometric detector).

The preparation of ^{18}F-labelled PEG-thiol-acids was carried out by condensation of [^{18}F]**4** with the corresponding α-Thio-ω-carboxy poly (ethylene glycol) (MWs of 458.6 and 3300 Da). These experiments were conducted to have a proof of principle of the feasibility of the condensation reaction, to be translated later on to the radiolabeling of block co-polymers P and 3P (*vide infra*). The coupling reaction (see Figure 3 for PEG-thiol-acid with MW=458.6 Da) was optimized by using different temperatures and reaction times, and the radiochemical conversion (RCC) was determined by direct integration of the radiometric chromatographic profiles at different reaction times. For the low MW PEG-thiol-acid, RCC values at 90°C reached a plateau (>90% RCC) at t>10 min. A similar kinetic profile was also observed at T=70°C, although lower conversion values (<85%) could be achieved and the plateau was slightly delayed (t>20 min). Very similar results were obtained for the higher MW PEG-thiol-acid.

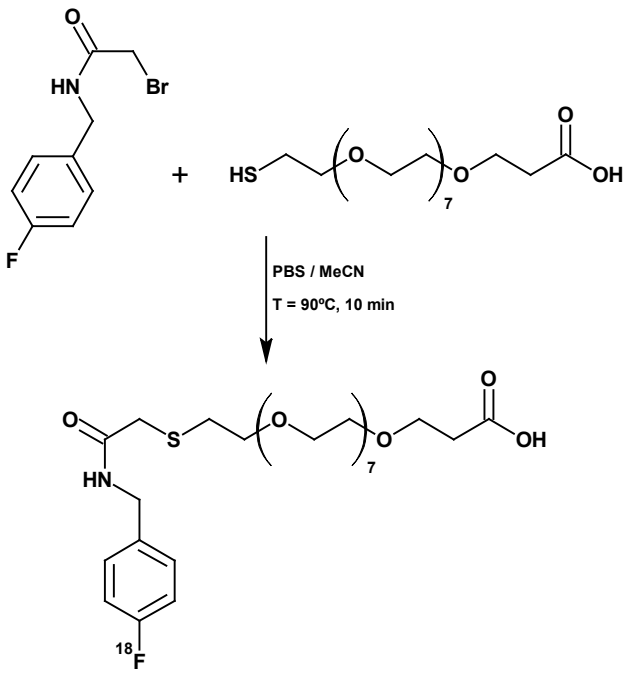

Figure 3 Synthesis of [^{18}F]-FBBA-PEG-thiol-acid by the condensation of [^{18}F]FBBA with PEG-thiol-acid with Mw 458.6 Da

Large scale synthesis under optimal conditions resulted in overall radiochemical yields (referred to [^{18}F]FBBA) of 51±7% (uncorrected) after purification. UPLC-ESI/MS and MALDI-TOF-MS analysis of the collected fractions confirmed the presence of the condensation products. Major peaks at m/z = 624.3 ($M + H^+$) and 641.3 ($M + NH_4^+$) were detected for low MW PEG-thiol acid and m/z = 1691.26 for high MW PEG-thiol acid, the latter corresponding approximately to half of the molecular weight of the condensation product.

The first and second strategies used for the preparation of radiolabelled NPs (*vide infra*) required the preparation of radiolabelled block co-polymers P and 3P (namely, [^{18}F]P and [^{18}F]3P). Incorporation of the labelled active agent [^{18}F]FBBA into block-co polymers P and 3P was carried out following the chemical reaction schematized in Figures 4 and 5, respectively. Radiochemical conversion values of 52% and 65% were achieved for polymer P at 90°C and 120°C, respectively. However, at 120°C the reaction occurred faster, reaching a plateau after 30 minutes. The plateau was reached only after 120 min when the reaction was conducted at 90°C. For 3P block co-polymer, radiochemical conversion was approximately 60% after 1 hour when the reaction was carried out at 120°C. After

purification by HPLC, [^{18}F]P and [^{18}F]3P could be obtained in overall decay-corrected radiochemical yields of 17 ± 4% and 27± 7%, respectively, referred to the starting amount of [^{18}F]FBBA.

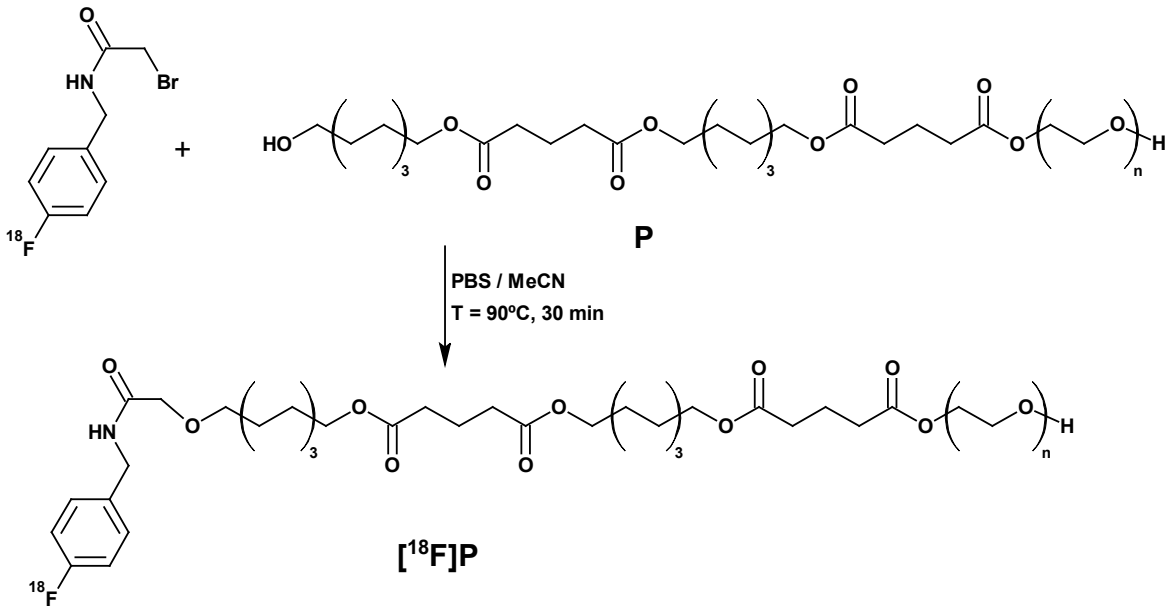

Figure 4 Synthesis of [^{18}F]FBBA-P block co-polymer ([^{18}F]P)

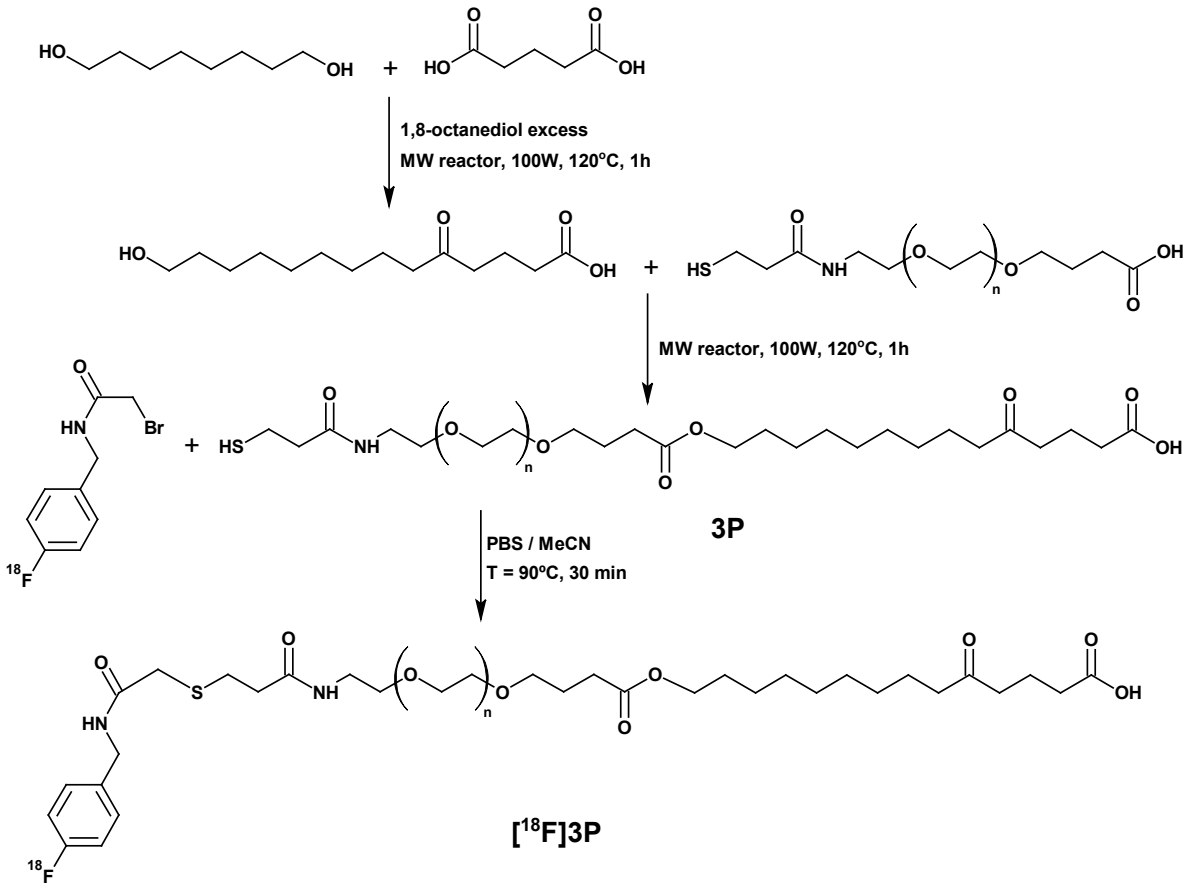

Figure 5 Synthesis of [^{18}F]FBBA-3P block co-polymer ([^{18}F]3P)

Synthesis and characterization of [^{18}F]-labeled NPs

In a previous work we have developed a peptide-targeted nano system able to modulate and control the release of PTX across an *in vitro* BBB model based on human glioma cells (results pending from publication). Here, by modifying the nano co-precipitation method, ^{18}F-labeled/peptide-functionalized NPs were obtained following three different methods as specified in the experimental section (see Figure 6 and Materials and Methods section for the preparation of 2P). These three strategies resulted in values of radiolabeling efficiency (R.E.) ranging from 5 to 14 %, related to the amount of starting radiolabelled polymer (strategies 1 and 2) or starting amount of [^{18}F]FBBA (strategy 3) (Table 1).

According to the measurements of particle size and zeta potential, the incorporation of the radiolabel did not result in statistically significant alteration of the physic-chemical properties of the resulting NPs. All the formulations exhibited average diameters in the desired range (below 200 nm) with a narrow size distribution (polydispersity ranging from 0.05 to 0.282). Moreover, all formulations exhibited a net negative charge with zeta-potential values approximately of -30 mV.

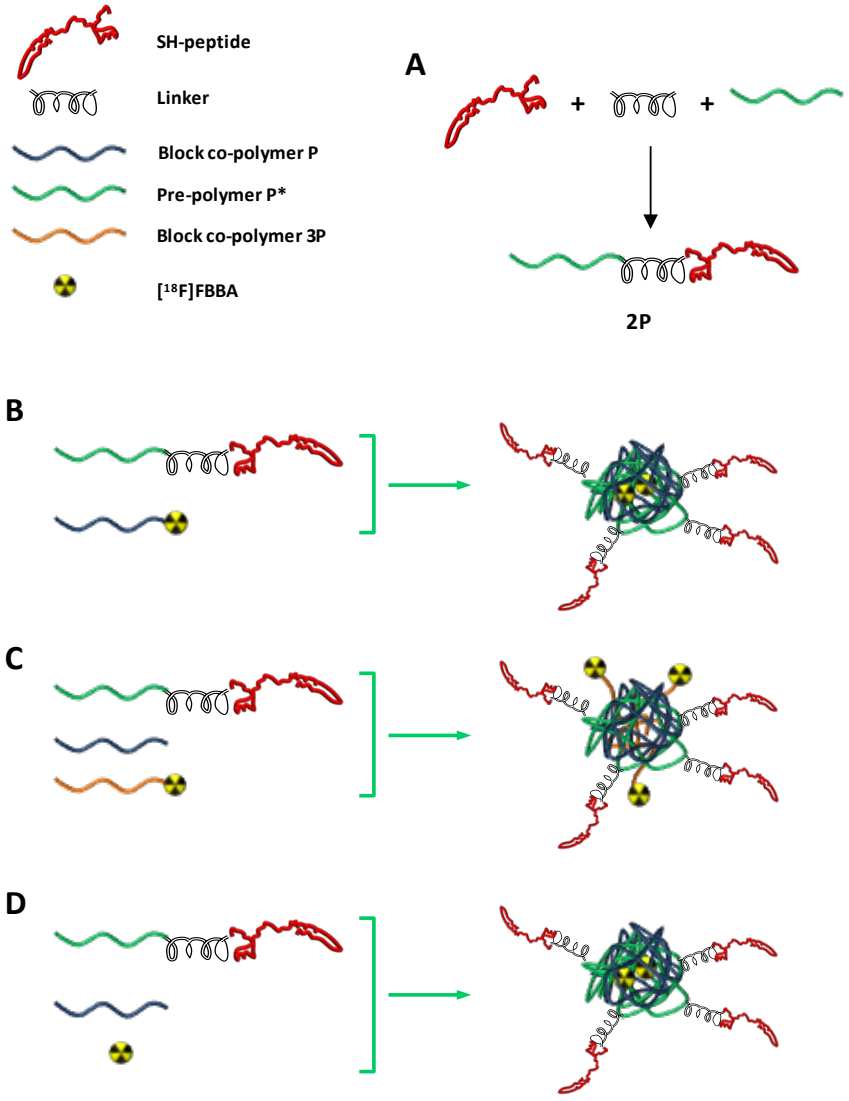

Figure 6 (A) Schematic illustration of the three strategies employed for the fabrication of ^{18}F-labeled and peptide-functionalized-NPs via co-precipitation. Labelled parts are (B) block co-polymer P (strategy 1), (C) block co-polymer 3P (strategy 2) and (D) entrapped [^{18}F]FBBA (strategy 3).

Radiochemical stability studies showed no detachment of the radioactivity for NPs prepared following strategies 1 and 2 (radiochemical purity > 95% after 12 hours). Slow detachment of [^{18}F]FBBA was observed at long times for NPs synthesized following strategy 3. As shown in a previous study,[25] degradation of the NPs may occur during the first days through uniform bulk degradation of the matrix. However, the relatively fast detachment of [^{18}F]FBBA could be attributed to a simple diffusion process through the polymer core matrix, as a result of water penetration.

Table 1 R.E. (%) for the NPs obtained by different strategies (radionuclide anchored to polymers P and 3P, and encapsulation of [^{18}F]FBBA).

^{18}F-labelling strategy	**Radiolabelling efficiency (%)**
[^{18}F]P	5 ± 2
[^{18}F]3P	14 ± 3
[^{18}F]FBBA	10 ± 2

In vivo biodistribution in rats (PET-CT Imaging)

In vivo biodistribution studies using PET imaging were carried out using the labelled NPs prepared according to strategy 2 (this is, using [^{18}F]3P as labeled precursor). This decision was made based on radiochemical yields during particle preparation (see Table 1) and stability studies. The labelled precursors (namely, [^{18}F]FBBA and [^{18}F]3P) were also investigated as controls. PET dynamic images were acquired after intravenous administration of the labelled species and quantified by drawing volumes of interest (VOIs) on the CT images for selected organs (i.e. kidneys, liver, stomach and brain).

Figure 7 displays the percentage of injected dose per gram of tissue (%ID/g) obtained after analysis of the PET data. As can be seen, [^{18}F]FBBA showed a high uptake in the brain a short times after administration, followed by a progressive wash-out at t>16 minutes. Such high uptake may be due to the hydrophobic character of the molecule. [^{18}F]FBBA also

showed significant uptake in the liver (approximately 10%ID/g at 9 min < t < 37 min) and in the stomach, while accumulation in the kidneys was lower than accumulation observed for [^{18}F]3P and [^{18}F]NPs. This suggests a preferential hepatobiliary elimination pathway in combination with renal excretion. Significant accumulation in the lungs (not shown in Figure 7) was also observed, especially at short times after administration. This accumulation decreased over time, although at long times the presence of radioactivity in the lungs could still be detected (see Figure 8A for PET-CT images).

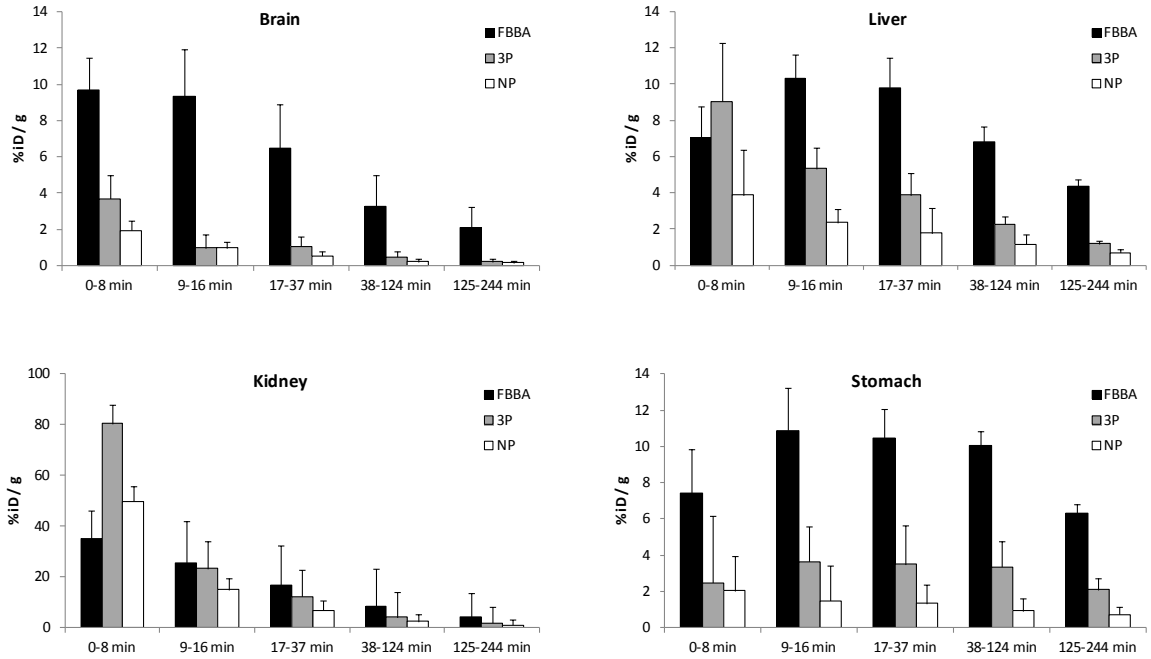

Figure 7 Accumulation of [^{18}F]FBBA (FBBA in the figure), [^{18}F]3P (3P in the Figure) and ^{18}F-labelled NPs (NP in the Figure) in brain, liver, kidneys and stomach, expressed as percentage of injected dose (%ID) per gram of organ (mean ± standard deviation, n=3) at different time points after intravenous administration.

[^{18}F]3P showed low accumulation in the brain with fast wash-out and very high accumulation in the kidneys, although uptake in the liver and the stomach was also significant. Again, this suggests elimination via the hepatobiliary system in combination with renal excretion.

Interestingly, labeled NPs showed a low accumulation in the liver and elimination mainly via urine. Actually, when NPs are administered, a variety of plasma proteins (e.g. opsonins) tend to bind to their surfaces. The conjugates can then be recognized by the MPS and internalized in macrophages, leading to a significant loss of NPs from circulation. The

decoration of the NPs with a PEG layer prevents opsonisation and sequestration by the MPS, resulting in prolonged blood circulation.[27,28] Hence, our results are in good agreement with the fact that renal excretion of the NPs becomes the preferred route when the NPs are surface-functionalized with PEG; despite the negative superficial charge of the developed peptide-functionalized-NPs, which favours the interaction with the MPS, opsonization and consequently liver accumulation was clearly avoided thanks to stealthy behaviour awarded to our nanoparticulate system. The low accumulation in the liver should also prevent hepatotoxicity, which might be a consequence of high liver uptake.[29]

Contrary to NPs, a marked renal uptake for [^{18}F]3P block co-polymer was observed. These results confirm that low molecular weight block co-polymers have a major tendency to be eliminated via urine, contrary to larger molecules or NPs.[29] Of note, the differences in the uptake values obtained for [^{18}F]3P and [^{18}F]NPs suggest the chemical and radiochemical stability of the NPs *in vivo*, at least during the duration of the study. As shown in Figures 7 and 8, a low accumulation of NPs was observed in the brain despite the presence of the peptide. The low uptake observed at short times after administration might be due to the contribution of the presence of labeled NPs in the blood, and hence animal sacrifice, organ removal and subsequent determination of the amount of radioactivity using a gamma counter may provide more accurate information about the real concentration of NPs in the brain. However, due to invasiveness of the technique, different animals should be utilized to obtain uptake values at different time points after administration.

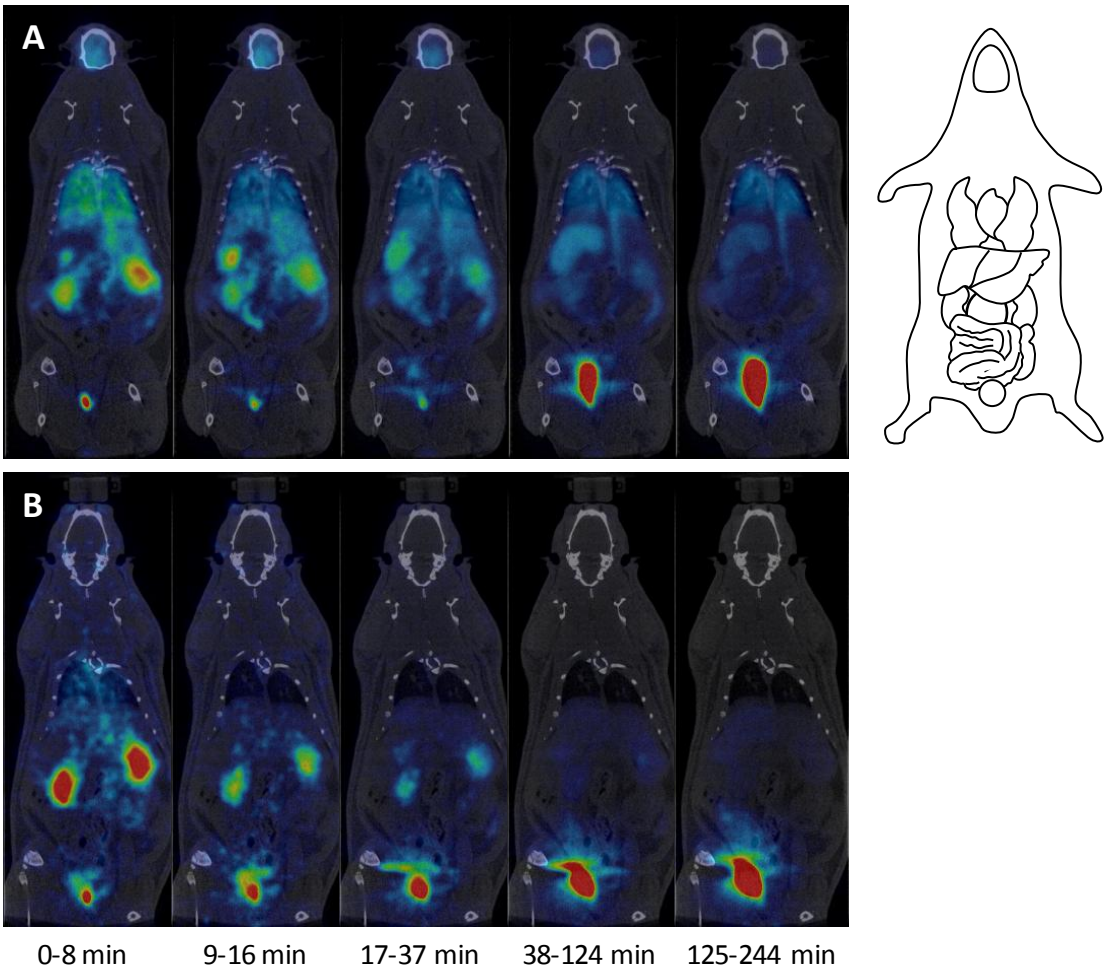

Figure 8. PET images (Maximum intensity projections) for [^{18}F]FBBA (A) and [^{18}F]NPs (B) at different time points after administration. Frames within each time-gap have been averaged to create the images displayed. Computerised tomography (CT) images were adjusted along the Y axis for an appropriate fitting with the tracer distribution image.

EXPERIMENTAL PROCEDURES

The experimental part of this work has been carried out in the Molecular and Functional Imaging Facility of CIC biomaGUNE. 1,8-Octanediol (98%), 2,2'-dithiodipyridine (≥97%) and polyethyleneglycol (PEG, Mw 1.5 KDa) were purchased from Sigma (Sigma–Aldrich, USA). Glutaric acid (99%) was obtained from Alfa Aesar (USA). AGBBB015F (CGGKTFFYGGSRGKRNNFKTEEY)) peptide, fluorescently labeled with carboxyfluorescein, was synthesized by Innovagen AB (Sweden). PEG Thiol acids, α-Thio-ω-carboxy poly (ethylene glycol) (MW 458,6 and 3.300 Da) were supplied by Iris Biotech GmbH (Germany). Ultrapure water (Type I water, ISO 3696) was obtained from a Milli-Q®

system (Merck Millipore). All other chemicals, unless otherwise specified, were of analytical grade and were purchased from Sigma (Sigma–Aldrich, Germany).

Synthesis of the ^{18}F-labeled prosthetic group [^{18}F]FBBA

The prosthetic group 4-[^{18}F]fluorobenzyl-2-bromoacetamide ([^{18}F]FBBA, [^{18}F]**4**, Figure 1) was synthesized following a previously reported methodology[26] with minor modifications. 4-[^{18}F]fluorobenzonitrile ([^{18}F]**2**) was prepared by reaction of 4-Cyano-*N*,*N*,*N*-trimethylanilinium trifluoromethanesulfonate (**1**) with [^{18}F]F^- generated by proton irradiation of [^{18}O]H_2O (>98%, Rotem Industries Ltd.); [^{18}F]F^- was first trapped in an anion exchange resin and subsequently eluted with K_2CO_3/H_2O and Kryptofix2.2.2/MeCN. After azeotropic evaporation of the solvent, the dried potassium [^{18}F]fluoride-Kryptofix2.2.2 complex was dissolved in dry DMSO and the resulting solution was reacted with **1** (130ºC, 10 min). The reaction mixture containing [^{18}F]**2** was cooled, diluted with purified water (9 mL) and flushed through a C-18 cartridge (Sep-Pak®, Waters). The retained labeled species was eluted with 2.5 mL of THF, dried over Na_2SO_4 and molecular sieve and reacted with $LiAlH_4$ in THF (120°C, 2 min) to yield [^{18}F]**3**, which was further reacted with bromoacetyl bromide (solution in CH_2Cl_2). After addition of 2 mL of MeCN/water 1/1, the mixture was purified by high performance liquid chromatography (HPLC) using a VP125/10 Nucleosil 100-7C18 semipreparative column (Macherey-Nagel) as stationary phase and MeCN/water 1/1 as the mobile phase to yield [^{18}F]**4** (retention time = 13 min) in overall yield of 12% (decay corrected). The collected fraction was used without further treatment for subsequent labeling steps. The presence of the desired product was confirmed by HPLC and co-elution with reference standard, using an Agilent 1200 Series HPLC system with a multiple wavelength UV detector (λ = 254 nm) and a radiometric detector (Raytest). A RP-C18 column (Eclipse XDB C18, 4.6x150 mm, 5 μm particle size) was used as stationary phase and water/MeCN (60/40) was used as the mobile phase at a flow rate of 1 mL/min (retention time = 9.5 min, injected volume = 20 μL).

Synthesis of ^{18}F-labeled PEG-thiol-acids

The preparation of ^{18}F-labelled PEG-thiol-acids was carried out by condensation of [^{18}F]**4** with the corresponding α-Thio-ω-carboxy poly (ethylene glycol). These experiments were

conducted to have a proof of principle of the feasibility of the condensation reaction, to be translated later on to the radiolabelling of block co-polymers P and 3P (*vide infra*). Experimentally, a 1 mg/mL solution of PEG-thiol-acid in 1:1 (v/v) phosphate buffer saline and acetonitrile (total volume = 250µL), was mixed with a solution of [^{18}F]FBBA in water/MeCN (1/1, 250 µL). Two different PEG-thiol-acids with molecular weights of 458.6 (Figure 3) and 3300 Da were used, and experimental conditions were optimized (T = 70-90°C, t=10-30 min) in both cases. The radiochemical conversion (RCC) was determined by radio-HPLC, using the same experimental conditions as above.

Large scale syntheses were carried out using the optimal reaction conditions (T= 90°C, t = 10 min); the radiolabelled species were purified by HPLC under analytical conditions described above using a 500 µL injection loop. The fractions containing the pure labelled polymers were collected, allowed to complete decay and the identity of the labelled species was confirmed by UPLC/ESI-MS (low MW PEG-thiol-acid) or MALDI-TOF-MS (high MW PEG-thiol-acid). UPLC-MS analyses were performed using an AQUITY UPLC separation module coupled to a LCT TOF Premier XE mass spectrometer (Waters, Manchester, UK). An Acquity BEH C18 column (1.7 µm, 5 mm, 2.1 mm) was used as stationary phase. The elution buffers were A (water and 0.1% formic acid) and B (Methanol and 0.1% formic acid). The column was eluted with a gradient: t=0 min, 95% A, 5% B; t=0.5 min, 95% A, 5% B; t=7.5 min, 1% A, 99% B; t=10min, 1% A, 99% B. Total run was 10 min, injection volume was 5 µL and the flow rate 300 µL/min. The detection was carried out in negative ion mode, monitoring the most abundant isotope peaks from the mass spectra. For MALDI-TOF-MS analyses, the sample preparation was carried out by deposition of 0.5 µL of sample directly onto a pre-spotted Anchorchip (PAC-II 96, Bruker Daltonics) plate that contains α-cyano-hydroxycinnamic acid matrix (HCCA). MALDI-TOF analysis was performed using an UltrafleXtreme III time-of-flight mass spectrometer equipped with a Nd:YAG laser (Smartbeam II, 355 nm, 1 kHz) and controlled by Flex Control 3.3 software (Bruker Daltonics, Bremen, Germany). The acquisitions were carried out in positive-ion reflectron mode at a laser frequency of 500 Hz. The spectrum was acquired at 30% laser fluency and was recorded in the m/z range from 1400 to 2000. The deflector cutoff was set at m/z 1000 and the spectrum resulted from accumulation of 1000 laser shots.

Synthesis of ^{18}F-labeled P block co-polymer ([^{18}F]P)

The first strategy for the synthesis of radiolabelled NPs required the preparation of radiolabelled block co-polymer P, which was prepared by the esterification of 1,8-octanediol with glutaric acid and subsequent reaction with PEG 1500. Glutaric acid (6 g, 45 mmol) and 1,8-Octanediol (5.53 g, 37 mmol) were reacted in a microwave reactor (Discovery CEM) at 100 W for 1 hour. The reaction was performed under vacuum (100 mbar) with continuous stirring by air-cooling to maintain the temperature constant at 120°C to form the pre-polymer. Subsequently, PEG 1500 was added (1:1 weight ratio with the pre-polymer) and the polymerization reaction was conducted in the microwave reactor with the conditions described above (100 W, 1 hour) to yield P as a white solid.

For the radiosynthesis of [^{18}F]FBBA-labeled P block co-polymer ([^{18}F]P), a 1 mg/mL solution of P in 1:1 (v/v) phosphate buffer saline and acetonitrile (total volume = 250 μL), was mixed with an equal volume of a solution of [^{18}F]FBBA in water/acetonitrile (Figure 4). The reaction was incubated at a pre-determined temperature and the radiochemical conversion was monitored at different times from chromatographic profiles (chromatographic conditions described above). Different incubation times (30, 60, 90 and 120 min) and temperatures (90°C and 120°C) were tested in order to achieve optimal reaction conditions.

Large scale syntheses for *in vivo* experiments were carried out using the optimal reaction time (30 min) and temperature (90°C); the radiolabelled species was purified by HPLC under conditions described above, using a 500 μL injection loop.

Synthesis of ^{18}F-labelled 3P block co-polymer ([^{18}F]3P)

The second strategy for the preparation of radiolabelled NPs (vide infra) required the preparation of a novel block co-polymer (3P) labeled with ^{18}F (Figure 5). First, the microwave-assisted production of a pre-polymer (P*) was approached by reacting glutaric acid and 1,8-octanediol at a molar ratio of 1:1.2 at 100 W for 1 hour. The reaction was performed under vacuum with continuous stirring and air-cooling to maintain the temperature at 120°C. The resulting pre-polymer P*, which contained an excess of 1,8-octanediol, was reacted with the PEG-thiol-acid (3.3 KDa) to obtain 3P block co-polymer. This second reaction was conducted in a microwave reactor under experimental conditions

described above (100 W, 1 hour), using a 1:1 (w/w) ratio between P* and PEG-thiol-acid. Finally, radiolabeling of 3P was achieved by condensation with [^{18}F]FBBA, under the same experimental conditions used for the preparation of ^{18}F-labelled PEG-thiol-acids.

Synthesis of block co-polymer 2P

In order to achieve targeted NPs, a block co-polymer attached *via* a linker to peptide AGBBB015F was used during NP preparation. AGBBB015F (15F), introduced in 2007 by Demeule and co-workers[30], is a peptide that belongs to a family of peptides named Angiopeps, which were derived from the Kunitz domain of aprotinin. Angiopeps are known to be able to pass through the BBB via a mechanism which involves the LDLR (low density lipoprotein receptor).

For the preparation of the linker, 2,2'-dithiodipyridine (MW:220.31, 66.4 mg, 2.14 mmol) in THF (5 mL) and AcOH (5 mL) were added to an oven dried one-necked flask under nitrogen atmosphere. α-Thio-ω-carboxy poly (ethylene glycol) (MW 3317 Da, 500 mg, 1.07 mmol) dissolved in THF was added dropwise and the solution was allowed to stir for three days. The product was then precipitated by addition of hexane (100 mL) under low magnetic stirring. The solution was refrigerated overnight at 8-10°C, and subsequently vortexed and centrifuged (two cycles, 2700 g, 15' and 1300 g, 20'). After each cycle the supernatant was removed, the same amount of hexane was added and a short vortex agitation to redisperse the pellet was performed. Residual solvent was removed under vacuum to yield the product as a yellow solid.

The coupling between Cysteine residues present at AGBBB015F and linker was carried out in 5 ml PBS (10 mM, pH 7.4). Linker and peptide (1:1.05 molar ratio) were accurately mixed and the reaction was stirred at 0 °C for 4 hours to reach quantitative conversion. The solution was finally lyophilized to yield Peptide-Targeted Linker as a white powder.

Finally, to obtain the block co-polymer 2P, a preliminary step for the production of the pre-polymer P* was needed. Glutaric acid and 1,8-octanediol (molar ratio of 1:1.2) were reacted under microwave heating at 100 W for 1 hour. The pre-polymer P*, containing an excess of 1,8-octanediol, was reacted with the linker bearing AGBBB015F in the microwave reactor under identical conditions to those described above and using a ratio 1:1

(w/w) between preformed peptide-targeted linker and pre-polymer P*. The resulting targeted block co-polymer was obtained as a white solid.

Synthesis and characterization of [^{18}F]-labeled/peptide-functionalized NPs

The synthesis of ^{18}F-labelled/peptide functionalized NPs was approached following a previously reported nano co-precipitation method,[25] with some modifications. Three different strategies were followed, depending on the labelled species used. In all of them, peptide-functionalized block co-polymer 2P (Figure 6A) was used as one of the starting materials. The first strategy (Figure 6B) consisted of dissolving block co-polymers [^{18}F]P and 2P at 9:1 (w/w) ratio in 1 ml of acetone to form the diffusing phase. This phase was then added to 20 ml of ultrapure water by means of a syringe controlled by a syringe pump (KD Scientific) under magnetic stirring at room temperature; the needle was positioned directly in the medium and a flow rate of 50 μL/min was used. The resulting suspension was allowed to stir uncovered, in order to allow the evaporation of acetone. The suspension was purified by centrifugation (Hettich Centrifuge, EBA 21, 4000 g, 45 min at RT) with ultracentrifugal filters (Amicon Ultra-15, Ultracel membrane with 100.000 MWCO, Millipore, USA). The second strategy (Figure 6C) consisted of dissolving block co-polymers P, 2P and [^{18}F]3P in the organic phase (acetone) at a ratio 8:1:1 (w/w), and following exactly the same experimental procedure. Finally, and taking advantage of the hydrophobic character of the labelled prosthetic group, a third strategy (Figure 6D) consisting of encapsulating [^{18}F]FBBA into the peptide-functionalized NPs was approached. With that aim, the labelled species ([^{18}F]FBBA) was dissolved in the organic phase (acetone, 1 mL) together with the starting polymers (P and 2P), and the solution was added dropwise to the aqueous phase under continuous stirring, following the same experimental procedure.

In all cases, the physicochemical properties (size and zeta potential) of the resulting ^{18}F-labeled/peptide-functionalized NPs were determined after complete decay as described in our previous work.[25] To assess the radiolabeling efficiency (R.E., %), the amount of radioactivity in the pellet and the supernatant after centrifugation were determined, and R.E. was calculated as the ratio between the amount of radioactivity in the pellet and total amount of radioactivity (pellet + supernatant).

To assess the radiochemical stability, NPs were prepared and purified as described above and subsequently resuspended in 200 µL of physiologic NaCl 0.9% solution (Braun Medical S.A.). The suspension was then divided into 3 different aliquots containing 50 µL of the NPs each. The aliquots were kept at 37°C for 1, 3 and 12 hours, respectively. The samples were then filtered (Amicon Ultra-15, 100.000 MWCO) and radioactivity was measured in a 2470 WIZARD2 Automate Gamma Counter (PerkinElmer). The dissociation of ^{18}F (expressed in percentage) at each time point was calculated as the ratio between the amount of radioactivity in the filtrate (decay-corrected) and the starting amount of radioactivity.

Animals

Healthy, 9-10 weeks aged Sprague-Dawley rats (Harlan, Udine, Italy) were used to examine the biodistribution pattern of radiolabelled NPs after intravenous injection. The animals were maintained and handled in accordance with the Guidelines for Accommodation and Care of Animals (European Convention for the Protection of Vertebrate Animals Used for Experimental and Other Scientific Purposes) and internal guidelines, and experimental procedures were approved by the local authorities. Rats were acclimated to the housing facility at 22-24°C and 40-60% of humidity under light/dark conditions for at least 5 days prior to experiments.

In vivo biodistribution in rats (PET-CT Imaging)

Animals were anesthetized with 4.5% isoflurane in pure oxygen as carrier gas. ^{18}F-labelled NPs were suspended in a certain volume of saline solution (NaCl 0.9%) to obtain the required concentration of radioactivity (37-74 MBq/mL) and intravenously administered via one of the lateral tail veins. Formulations of ^{18}F-3P and ^{18}F-FBBA were also administered and used as controls.

PET-CT imaging was performed on an eXplore Vista-CT camera (GE Healthcare). Acquisition of the scans was started immediately after dose administration. Three beds were defined to acquire whole body images (frames: 4 x 4 min, 4 x 7 min, 4 x 20 min, 4 x 30 min, total acquisition time = 244 min). After acquisition, a CT scan was performed for

later attenuation correction during image reconstruction. Random and scatter corrections were also applied to the reconstructed images (2DOSEM iterative algorithm, 4 iterations). PET-CT images were co-registered and analyzed using PMOD image processing tool. Volumes of interest (VOIs) were drawn in the kidneys, liver, stomach and brain, using the CT images for anatomical reference. Time–activity curves (decay corrected) were obtained for each organ as cps/cm^3. Curves were transformed into real activity (Bq/cm^3) curves by using a calibration factor. Injected dose and organ mass normalizations were finally applied to data to achieve percentage of injected dose per gram of tissue (%ID/g).

CONCLUSIONS

This work describes a novel approach for the radiolabeling of PNPs and subsequent utilization for the *in vivo* determination of the biodistribution pattern using a combination of imaging techniques, i.e. Positron Emission Tomography (PET) and Computerized Tomography (CT). These techniques represent an ideal tool for investigations of pharmacological profiles of new nanosystems. The labeling approach is based on radiolabelling one of the precursor polymers, which is finally integrated in the NP using a nanoprecipitation method. Radiolabelled NPs showed values of size and zeta potential equivalent to those of the unlabelled analogues, within the experimental error. The labeled NPs enabled the quantification of the biodistribution data in rats up to 4 hours after intravenous administration. PET images show low accumulation in the liver and elimination mainly via urine. The different biodistribution pattern obtained for the "free" radiolabelled polymer ([^{18}F]3P) suggest chemical and radiochemical integrity of the NPs under investigation.

The strategy reported here might be applied to the preparation of other radiolabelled polymeric NPs, in order to determine their pharmacokinetic properties and evaluate their potential therapeutic capabilities.

ACKNOWLEDGMENTS

The authors would like to thank GEMAT group of IQS for preliminary synthesis work, Sagetis-Biotech for promoting the investigation, Mikel González and Mikel Errasti for radioisotope production and radiochemical synthesis, Maria Puigivila for technical assistance during *in vivo* experiments and image analysis and Dr. Javier Calvo for assistance in mass spectrometry. The *in vivo* work was partially funded by Ministerio de Economía y Competitividad (Project reference MAT2013-48169-R).

ABBREVIATIONS

[^{18}F]FBBA, 4-[^{18}F]fluorobenzyl-2-bromoacetamide; UV, ultraviolet; PEG-thiol-acid, α-Thio-ω-carboxy poly (ethylene glycol); RCC, radiochemical conversion; HPLC, high-performance liquid chromatography; UPLC, ultra-performance liquid chromatography; ESI, electrospray ionization; MS, mass spectroscopy; TOF, time of flight; THF, tetrahydrofuran; AcOH, acetic acid; PBS, phosphate buffer solution; MW, molecular weight; MWCO, molecular weight cut-off; PTX, paclitaxel; BBB blood-brain barrier; MPS, mononuclear phagocyte system; RES, reticuloendothelial system.

REFERENCES

(1) A. Guerrero-Martínez, S. Barbosa, I. Pastoriza-Santos LML-M.(2011) Nanostars shine bright for you. Colloidal synthesis, properties and applications of branched metallic nanoparticles. *Curr. Op. Colloid Interface Sci.* 16(118-127).

(2) M. Grzelczak, J. Pérez-Juste, P. Mulvaney LML-M.(2008) Shape Control in Gold Nanoparticle Synthesis. *Chem. Soc. Rev.* 37:1783-1791.

(3) C. Blasco and Y. Picó.(2011) Determining nanomaterials in food. *Trac-Trends Anal. Chem.* (30):84.

(4) M. Zielecka, E. Bujnowska, B. Kępska, M. Wenda and MP.(2011) Antimicrobial additives for architectural paints and impregnates. *Prog. Org. Coatings,* 72(1-2):193-201.

(5) Stroyuk AL, Shvalagin VV, and Kuchmii SY.(2005) Photochemical synthesis and optical properties of binary and ternary metal–semiconductor composites based on zinc oxide nanoparticles. *J. Photochem. Photobiol. A Chem.* 173(2):185-194.

(6) J. Blyszko, W. Kiernozycki, N. Guskos, G. Zolnierkiewicz, J. Typek UN and MP.(2008) Study of mechanical properties of concrete with low concentration of magnetic nanoparticles. *J. Non-Cryst. Solids* 354:4514-4518.

(7) Zhang L, Gu FX, Chan JM, Wang AZ, Langer RS, and Farokhzad OC.(2008) Nanoparticles in Medicine : Therapeutic Applications and Developments. *Clin. Pharmacol. Ther.* 83(5):761-769.

(8) W. Han, K. M. McCreary, K. Pi, W. H. Wang, Y. Li, H. Wen JRC and RKK.(2012) Spin transport and relaxation in graphene. *J. Magn. Magn. Mater.* 324(4):369-381.

(9) Zhua S-C, Kai-Lun Yaoa B, Gaoa G-Y, and Nia Y.(2013) Spin-dependent transport in graphene nanoribbons adsorbed with vanadium in different positions. *Solid State Commun.* 155:40-44.

(10) Bhattacharyya SB and P.(2012) Recent developments on graphene and graphene oxide based solid state gas sensors. *Sens. Actuat. B-Chem* 173:1-21.

(11) L. Cui, T. Pu YL and XH.(2013) Layer-by-layer construction of graphene/cobalt phthalocyanine composite film on activated GCE for application as a nitrite sensor. *Electrochim. Acta* 88:559-564.

(12) S. M. Janib, A. S. Moses JAM.(2010) Imaging and drug delivery using theranostic nanoparticles. *Adv. Drug Deliv. Rev* 62(11):1052-1063.

(13) Shenoy DB1 AM.(2005) Poly(ethylene oxide)-modified poly(epsilon-caprolactone) nanoparticles for targeted delivery of tamoxifen in breast cancer. *Int. J. Pharm.* 293(1-2):261-270.

(14) Chan JM, Valencia PM, Zhang L, Langer R FO.(2010) Polymeric nanoparticles for drug delivery. *Methods Mol Biol* (624):163-175.

(15) Owens DE, and Peppas N a.(2006) Opsonization, biodistribution, and pharmacokinetics of polymeric nanoparticles. *Int. J. Pharm.* 307(1):93-102.

(16) Moghimi SM, Hunter a C, and Murray JC.(2001) Long-circulating and target-specific nanoparticles: theory to practice. *Pharmacol. Rev.* 53(2):283-318.

(17) H. M.(2001) The enhanced permeability and retention (EPR) effect in tumor vasculature: the key role of tumor-selective macromolecular drug targeting. *Ad. Enzym. Regul* 41(189-207).

(18) R. D.(2005) Targeting and intracellular delivery of drugs. In: Wiley-VCH, ed. *Encyclopedia of Molecular Cell Biology and Molecular Meidicne*. 2nd ed. We.; 2005:163-203.

(19) Reiner T, Keliher EJ, Earley S, Marinelli B, and Weissleder R.(2011) Synthesis and in vivo imaging of a 18F-labeled PARP1 inhibitor using a chemically orthogonal scavenger-assisted high-performance method. *Angew. Chem. Int. Ed. Engl.* 50(8):1922-5.

(20) Locatelli E, Gil L, Israel LL, Passoni L, Naddaka M, Pucci A, Reese T, Gomez-vallejo V, Milani P, and Matteoli M.(2012) Biocompatible nanocomposite for PET / MRI hybrid imaging.

(21) Nahrendorf M, Zhang H, Hembrador S, Panizzi P, Sosnovik DE, Aikawa E, Libby P, Swirski FK, and Weissleder R.(2008) Nanoparticle PET-CT imaging of macrophages in inflammatory atherosclerosis. *Circulation* 117(3):379-87.

(22) Devaraj NK, Keliher EJ, Thurber GM, Nahrendorf M, and Weissleder R.(2009) 18F labeled nanoparticles for in vivo PET-CT imaging. *Bioconjug. Chem.* 20(2):397-401.

(23) Guerrero S, Herance JR, Rojas S, Mena JF, Gispert JD, Acosta G a, Albericio F, and Kogan MJ.(2012) Synthesis and in vivo evaluation of the biodistribution of a 18F-labeled conjugate gold-nanoparticle-peptide with potential biomedical application. *Bioconjug. Chem.* 23(3):399-408.

(24) Santiago Rojas, Juan D. Gispert, Roberto Martin Sergio Abad CM, and Deborah Pareto, Victor MV, Mercedes Alvaro HG and JRH.(2011) Biodistribution of Amino-Functionalized Diamond Nanoparticles. In Vivo Studies Based on 18F Radionuclide Emission. (7):5552-5559.

(25) Di Mauro PP, and Borrós S.(2014) Development of high drug loaded and customizing novel nanoparticles for modulated and controlled release of Paclitaxel. *Pharm. Res.* 31(12):3461-77.

(26) Kuhnast B, Klussmann S, Hinnen F, Boisgard R, Rousseau B, Frste JP, Tavitian B, and Doll F.(2003) Fluorine-18- and iodine-125-labelling of spiegelmers. *J. Label. Compd. Radiopharm.* 46(13):1205-1219.

(27) Chen X, Park R, Shahinian AH, Bading JR, and Conti PS.(2004) Pharmacokinetics and tumor retention of 125I-labeled RGD peptide are improved by PEGylation. *Nucl. Med. Biol.* 31(1):11-19.

(28) Wu Z, Li Z-B, Cai W, He L, Chin FT, Li F, and Chen X.(2007) 18F-labeled mini-PEG spacered RGD dimer (18F-FPRGD2): synthesis and microPET imaging of alphavbeta3 integrin expression. *Eur. J. Nucl. Med. Mol. Imaging* 34(11):1823-31.

(29) Stockhofe K, Postema JM, Schieferstein H, and Ross TL.(2014) Radiolabeling of Nanoparticles and Polymers for PET Imaging. *Pharmaceuticals (Basel).* 7(4):392-418.

(30) Demeule M, Currie J-C, Bertrand Y, Ché C, Nguyen T, Régina A, Gabathuler R, Castaigne J-P, and Béliveau R.(2008) Involvement of the low-density lipoprotein receptor-related protein in the transcytosis of the brain delivery vector angiopep-2. *J. Neurochem.* 106(4):1534-44.